Experimental and Numerical Investigation of the Arms Displacement in a New Electrothermal MEMS Actuator

M. Kolahdoozan *
Department of Mechanical Engineering,
Najafabad Branch, Islamic Azad University, Najafabad, Iran
E-mail: mojtaba_kolahdoozan@yahoo.com
*Corresponding author

A. Rouhani Esfahani & M. Hassani
Department of Mechanical Engineering,
Najafabad Branch, Islamic Azad University, Najafabad, Iran
E-mail: amin.rouhany1367@gmail.com, m.hasanee@smc.iaun.ac.ir

Received: 19 January 2017, Revised: 8 February 2017, Accepted: 5 March 2017

Abstract: Microgrippers can be effectively applied for handling, positioning and assembling of the micro components. In the present study, a new design of a U-shape electrothermal microgripper was fabricated and developed with the voltages correspond between 1 to 10 volts. The microgripper was made of silicone with thickness of 25 microns, and pieces between 460 to 480 microns. The proposed microgripper has a simpler design and more facile fabrication comparing to most reported electrothermal microgripper. The behavior of the microgripper was simulated in COMSOL software to measure the displacement of the arms which hold and heat generations during the voltage changes. The present microgripper has more thermal and voltage tolerance comparing to other electrothermal microgripper. Furthermore, the obtained amount of tip displacement for voltage changes is acceptable. Another simulation method based on a three layer artificial neural network model (ANN) was carried out. Feed forward back propagation algorithm was employed as training algorithm to predict the displacement. The obtained results from both models proved that ANN model had better estimation due to the mean absolute percentage error of 1.024% and determination coefficient of 0.9995. Moreover, they confirm higher capability and accuracy of ANN in prediction of arms displacement compared to FEM.

Keywords: Artificial neural network, Electrothermal actuator, Finite element method, Micro electro mechanical system

Reference: Kolahdoozan, M., Rouhani Esfahani, A., and Hassani, M., "Experimental and Numerical Investigation of the Arms Displacement in a New Electrothermal MEMS Actuator", Int J of Advanced Design and Manufacturing Technology, Vol. 10 / No. 2, 2017, pp. 71-81.

Biographical notes: M. Kolahdoozan received his PhD in Mechanical Engineering from University of IAU Science and Research Branch in 2013. He is currently Assistant Professor at the Department of Mechanical Engineering, Najafabad University, Isfahan, Iran. His current research interest includes micro and nano electromechanical systems. **A. R. Esfahani** received his MSc in Mechanical engineering from Islamic Azad University of Najafabad in 2016. **M. Hassani** received his MSc in Mechanical engineering from Islamic Azad University of Najafabad in 2014. His current research interest includes Artificial Intelligent.

1 INTRODUCTION

In recent years, actuation, storage, and displacement techniques of MEMS (Micro Electro Mechanical System) have been deeply noticed [1-3]. Microgrippers and microsensors are some applications of MEMS [4-8]. Microgrippers have many applications in positioning and assembly of micro components [1], [6]. Therefore, different types of microgripper i.e. electrostatic [9], [10], electrothermal [11-13], electromagnetic [14-16] and piezoelectric [17] microgrippers have been considered. Hamedi et al., [18] designed and fabricated an electrostatic microgripping system using comb drive mechanism which predicted the displacement of the rotor and multi-field simulation of the electrostatic comb finger of the comb drive which was performed using finite element method. Bazaz et al., [19] presented a novel electrostatically actuated microgripper integrated with capacitive contact sensor. In order to investigate the mode shapes and natural frequencies of the microgripper, finite element analysis of the microgripper was performed in COVENTOR-WARE and the results were compared with analytical model. Thermal actuators have considerable advantages such as greater displacement at low voltages, robust structure, large output force, easy operation and easier fabrication compared with the other actuators. Nevertheless these actuators suffer from relatively high power consumption and low speed as the deflection [20], [21]. These actuators use the Joule heating and thermal expansion of materials to obtain mechanical actuation. Microgripper with electrothermal actuator is comprised of two micro-actuators (hot or thin and cold or wide arm actuator) therefore, when the voltage is applied to the structure, the passing electric current heats a thin arm and reclines to the wide arm [22].

Artificial neural network is one of the most applicable models for nonlinear analysis used in different aspects of MEMS and NEMS [23-27]. In recent years, ANN has been widely applied in different fields. Mehrabian and Aghil proposed a novel approach to optimize the location of piezoelectric actuators for vibration suppression of flexible structures. A flexible fin with bonded piezoelectric actuators was considered. Three multi-layer perceptron neural networks were employed to perform surface fitting to the discrete data generated by Finite Element Method (FEM). Invasive Weed Optimization (IWO), a novel numerical stochastic optimization algorithm, was utilized to maximize the weighted summation of Frequency Response Function (FRF) peaks. Results indicated an accurate surface fitting for the FRF peak data and an optimal placement of the piezoelectric actuators for vibration suppression was achieved [28]. Rabenorosoa et al., attached a piezoelectric microgripper with four degrees of freedom to a precision robot in order to enhance its dexterity and align the beam splitter to arcsecond angular tolerance. The modelling and control of the microgripper, and the alignment algorithm utilizing a novel spot-Jacobian servoing technique were discussed. Experimental results demonstrated the advantage of using the microgripper for optical alignment of the microspectrometer [29]. Ton presented a Radial Basis Function (RBF) neural network to predict rate-dependent hysteresis hybrid for piezoceramic actuator. The proposed hybrid hysteresis model consisted of hysteresis-like non-linearity in series with a dynamic RBF neural network used for implementing non-linear transformations of the phase lag and non-linear magnitude. The results indicated that the new modelling approach was very effective and have higher precision under a decayed input signal with the varying frequency [30]. Dong et al. investigated a new method for the identification of rate-dependent hysteresis in piezoceramic actuators. Both a so-called generalized gradient of the output with respect to the input of the hysteresis and the derivative of the input which represented the frequency change of the input were introduced into the input space. Moreover, the multilayer feed-forward neural network method was applied for modeling of the rate-dependent hysteresis. The experimental results on a piezoelectric actuator demonstrated promising results of the proposed approach [31].

In this research, U-shape microgripper with electro-thermal actuators was fabricated based on the chemical etching and vertical etching method. Then, COMSOL Multiphysics 4.4 software was applied for modeling and prediction of microgripper. Due to the high manufacturing costs and complex boundary conditions of the MEMS actuators, Multi physics powerful finite element software (COMSOL) was applied to simulate the microgripper behaviour and the performance of the fabricated microgripper such as displacements of arms hold and heat generations were evaluated. The obtained results showed good agreement between the experimental displacements of each micro-gripper arms and simulated displacements in COMSOL. Artificial intelligent simulation based on the neural network model was utilized for displacement prediction. Then, the results acquired from both models and experimental tests were compared in term of applied voltage.

2 MATERIALS AND METHODS

2.1. Microgripper Fabrication and Dimensions

Fabrication of microgripper consists of several steps that must be performed on both sides of the silicon wafer. Si<100> was used to fabricate microgripper, which comparing to other kinds (such as nickel) has the

advantages such as lack of back bending [32]. Another advantage of the proposed silicon (compared with metals) microgripper is later oxidation at high temperatures which lead to protect the structural function [32]. In this study, to fabricate the micro-electro-mechanical devices, Photo-lithography technique was used. According to this method, microgripper fabrication process consists of several steps, starting with chemical etching of the back side of Si wafer using Si3N4 mask and front side with vertical etching using Cr mask. Fig. 1 shows the photolithography masks used for both sides of the microgripper and Fig. 2 shows fabrication flowchart for microgripper. Fig. 3 represents the microgripper after completion of the etching process.

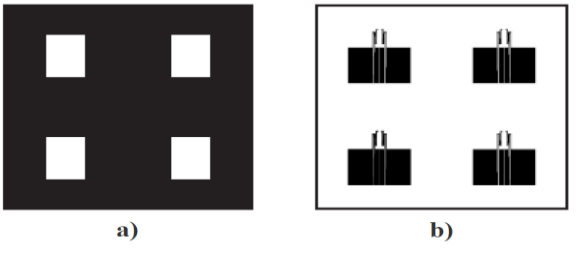

Fig. 1 Photolithography masks for a) chemical etching – back side of Si wafer and b) vertical etching – front side of Si wafer

a) Dicing the Si wafer

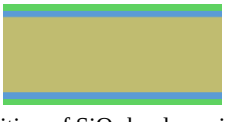

b) Deposition of SiO_2 by dry oxidation and Si_3N_4 by LPCVD (Low-Pressure Chemical Vapor Deposition) process

c) Deposition of Cr by E-beam evaporation on top of silicon wafer

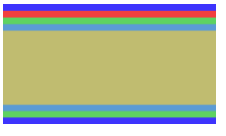

d) Deposition of positive photoresist by Spin coating

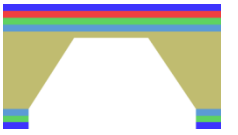

e) Etching of positive photoresist by lithography mask and Si_3N_4 by RIE (Reactive-ion etching). Chemical etching of SiO_2 using HF etchant and back side of Si using KOH etchant (475µm)

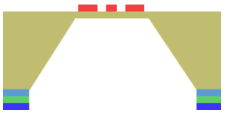

f) Chemical etching of Cr and vertical etching of front side of the Si wafer using Cr (25µm)

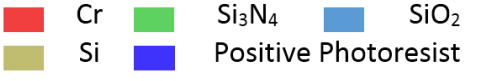

Fig. 2 Fabrication flowchart for microgripper

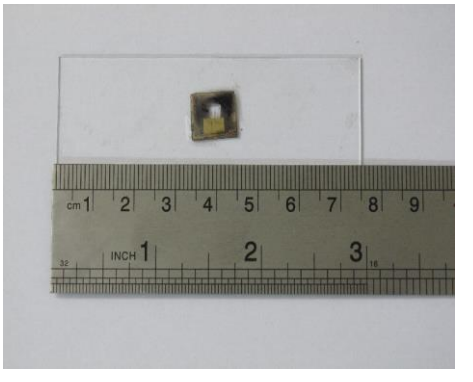

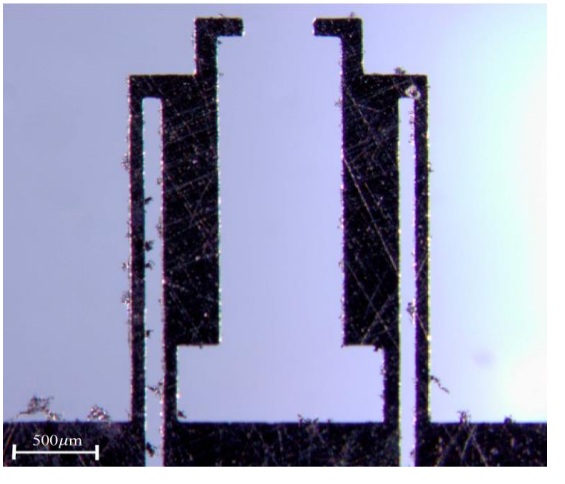

Fig. 3 The view of U-shaped microgripper after completion of the etching process

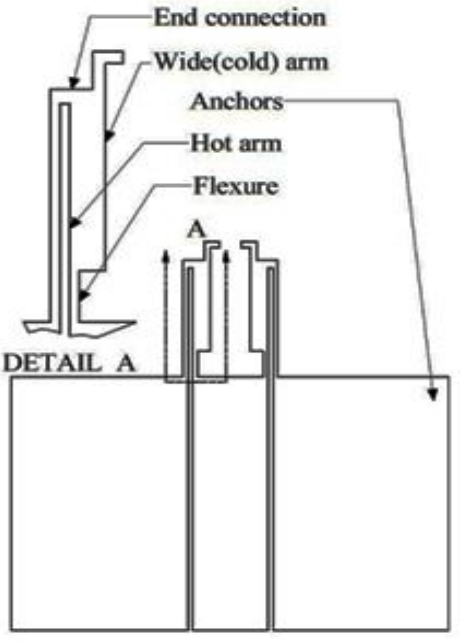

Fig. 4. The various components of the U-shape microgripper coupled in 2D

Table 1 Transitions selected for thermometry

Design Parameter	Hot arm		Wide(cold) arm		Flexure		End Connection		Anchors	
	Length	Width	Length	Width	Length	Width	Length	Width	Length	Width
Value[μm]	2860	100	2230	390	630	110	600	180	6230	3760

The various components of the microgripper are indicated in Fig. 4 and Table 1 summarizes final dimensions of the microgripper arms.

2.2. Finite element simulation

The COMSOL Multiphysics 4.4 software was used to analyze the U-shape microgripper based on the finite element analysis method. One of the advantages of using this software in comparison with the other simulation software is that the module of MEMS which is a collection of physics interfaces and predefined models, is incorporated in this package [33]. Schematic of the microgripper mesh model in finite element software is shown in Fig. 5 (a).

In this analysis, three different boundary conditions of structural, thermal and electrical conditions need to be investigated. Since the thermal boundary condition is more important and had a significant influence on the results, thus thermal analysis was considered in the simulation. In order to achieve the steady state, electrothermal actuators dissipate all of the electrical power of the input. At low temperatures, a significant amount of heat which is produced at the actuator, transmit through the pads to the substrate. But at higher temperatures (above 500 K), heat transfers by radiation and convection can play an important role [34]. This effect is more important when the desired actuator sizes are small. Fig. 5 (b) schematically shows the applied boundary conditions.

2.3. Material Properties

The structural material of the model is considered to be <1 0 0> oriented Si with 25 μm thickness. In finite element simulation of the desired actuator the mechanical properties and thermo-physical properties of the material (that are listed in Table 2 and Table 3) should be carefully selected and imported in to the models. Since the operating temperature of electrothermal actuators is high and the material properties are efficiently affected by the temperature, the properties such as thermal conductivity and thermal expansion coefficients must be considered as time-

varying variables. As Table 3 shows, the value of the coefficient of thermal conductivity of silicon changes significantly with the increment of the temperature.

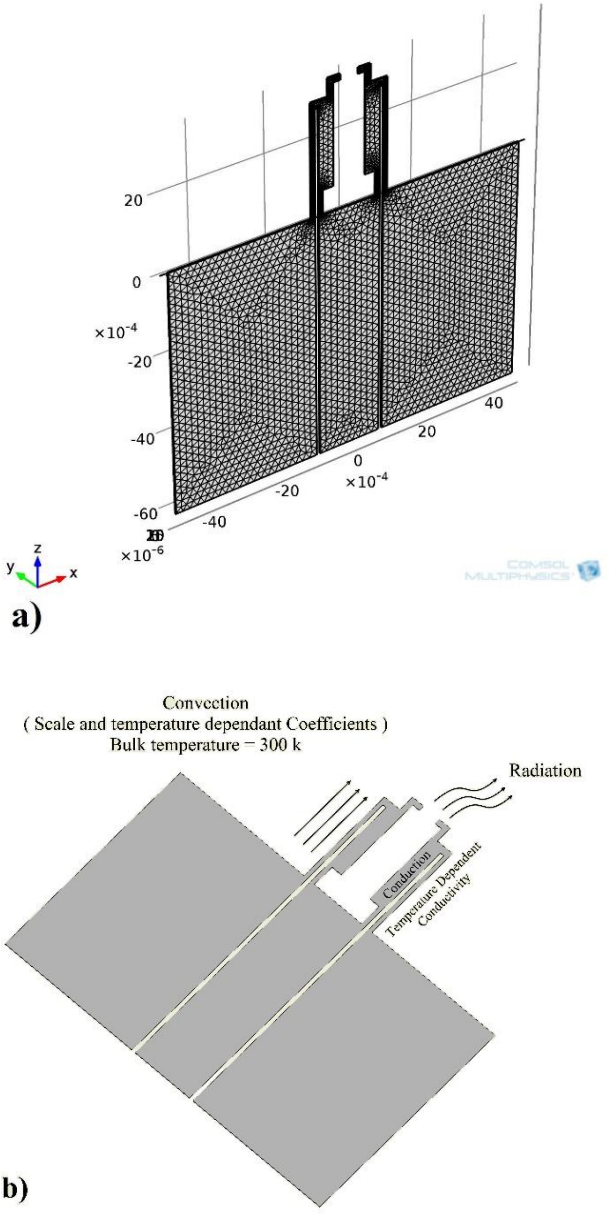

Fig. 5 a) Schematic of the microgripper mesh model b) Thermal boundary conditions applied in the finite element model

2.4. Artificial Neural Network

An ANN is a parallel processing network that has particular performance characteristics in common with biological neural networks [36]. The role of ANNs is to determine the complex nonlinear relationships between the parameters and to predict the output variables. ANN has generally three layers; input, hidden and output which interconnect parallelly. In ANNs, the input layer represents independent variables of the process and the output layer represents dependent variables of the process. Between them, hidden layers can be located. The number of neurons in input/output layers is the same as number of input/output variables, but the number of neurons in hidden layer should be obtained by trial and error [37], [38]. Fig. 6 shows the architecture of artificial neural networks. The input of each layer multiplies by special value to be called weight. These weights are selected randomly. The output of each layer is calculated by Eq.(1) [39].

Table 2 Thermophysical properties used in the simulation [34], [35]

Property	value
Heat capacity at constant pressure	678[J/(kg*K)]
Relative permittivity	4.5
Density	2329[kg/m^3]
Electrical onductivity	8200[S/m]
Young's modulus	169e9[Pa]
Poisson's ratio	0.3
Heat transfer coefficient	400[w/(m^{2}k)]
Thermal expansion	See Table. 3
Thermal conductivity	See Table. 3

Table 3 Variation of coefficient of linear thermal expansion α and thermal conductivity kt for Si in terms of temperature [34]

α (µm/ mK)	k_t (W/ mK)	Temperature (K)
2.568	146.4	300
3.212	98.3	400
3.594	73.2	500
3.831	57.5	600
3.987	49.2	700
4.099	41.8	800
4.185	37.6	900
4.258	34.5	1000
4.323	31.4	1100
4.384	28.2	1200
4.442	27.2	1300
4.500	26.1	1400
4.556	25.1	1500

$$Y = f\left(\sum X_j \, W_{ij} + b\right) \quad (1)$$

Where W_{ij} is the weight of the connection between each neuron (j) in input layer and each neuron (i) in hidden layer, and also between hidden and output layer. X_i is the value of the input (j) at the input layer, f is the transfer function and b is the bias.

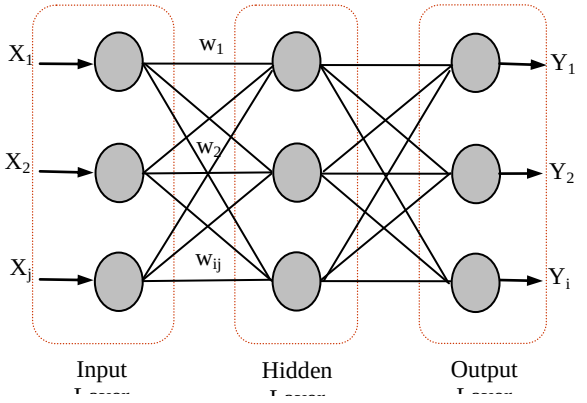

Fig. 6 Architecture of artificial neural network

In this study tan-sigmoid and purline function were used for hidden and output layers as transfer functions respectively. The equation of tan-sigmoid transfer function is as follow [40]:

$$f(x) = \frac{1}{1+exp(-x)} \quad (2)$$

Feed forward back propagation (FFBP) was used as training algorithm in the applied artificial neural network. All computations are carried out with MATLAB (version 7.10.0.499) mathematical software. Applied voltage was used as input variable and displacement of arms hold was used as output variable. 100 experimental points were employed to feed the model.

The data set was derived to training and test sets which contain 90 and 10 percent of data points respectively. According to the Eq. (3), all data points were to be scaled into the (-0.9,0.9) due to the use of the tan-sigmoid transfer function [40].

$$X_{norm} = 1.8 \frac{X - X_{min}}{X_{max} - X_{min}} - 0.9 \quad (3)$$

2.5. Statistical analysis

In order to analyze the obtained data, the paired t-test was applied in which the P-value of less than 0.05 was considered significant.

3 RESULTS AND DISCUSSION

Due to the direct correlation between the displacement of the tip of the microgripper for the different values of the applied voltage and the designed range of the actuator, the simulated (OR predicted) results were limited to the calculation of the displacement of the holder tip of the arms. In other words, for different parts in the range of microactuator, various displacements are required which are proportional to the input voltage. Hence, the input voltage can be achieved by understanding the amount of displacement required for hold operation. Due to the high working temperature of electrothermal microactuators, the temperature of the actuators used in the microclamping, especially in cases where the binding position of the parts are sensitive to high temperatures, must be precisely considered and determined. The results of the finite element solution for an input voltage of 10 V are shown in Fig. 7. As shown in the figure, the maximum displacement of the tip of the microgripper, for each arm is 10.072 µm.

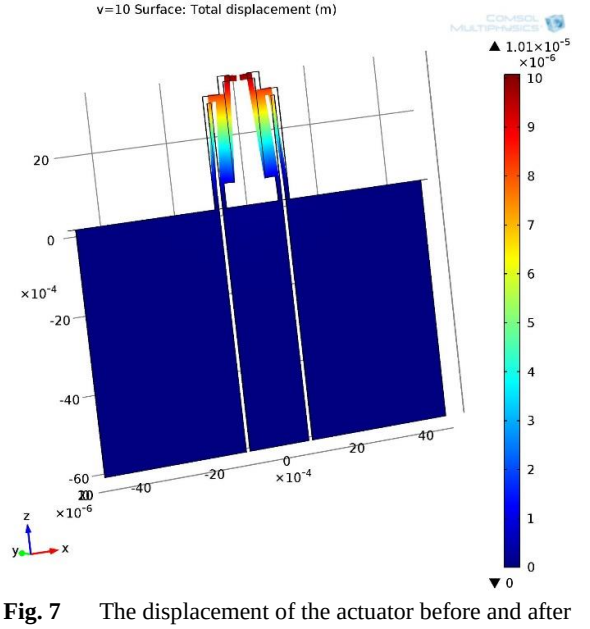

Fig. 7 The displacement of the actuator before and after applying voltage

In the design of the microclamps, the piece is hold from the place where two sides are in contact with the wide arms. Due to the high sensitivity of the pieces given position to the temperature, wide arm applied more force compared to thin arm to grab the pieces. In this state, because the pieces are in contact with wide arm, the temperature of the pieces will be equalized with the temperature of the environment and nor affected from the temperature of the thin arm.

The variation of temperature with voltage is plotted on the Fig. 8. As shown, the temperature increases non-linearly with voltage. The temperature of thin microgripper arm will be enhanced progressively proportional to the increment of the input voltage. This temperature will be led to the serious damage to the components that should be moved or positioned with the microgripper.

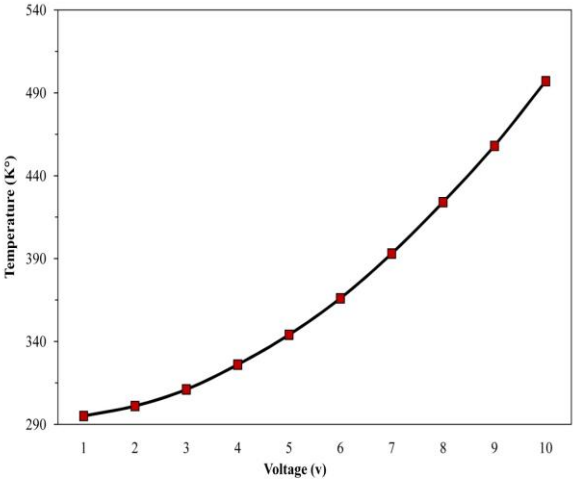

Fig. 8. The variation of temperature with voltage

The input variable of trained ANN is applied voltage and the output ones is displacement of arms hold. Topology of ANN is illustrated in Fig. 9. The number of layers, neurons of each layer and how to interconnect neurons between the layers are clearly shown in the present topology. The aim of training the ANN is to obtain the best weights with minimum values of prediction error. Table 4 illustrates the train data set which was implemented in training step.
Optimized ANN by considering minimum prediction error was obtained by changing the number of neurons in hidden layer, transfer functions and repetition of training step. In order to find the best number of neurons in hidden layer various topologies have been studied. Fig. 10 shows the error of each topology by changing the number of neurons in hidden layer. It can be seen that artificial neural network with 12 neurons in hidden layer has minimum value of mean square error (MSE). The equation of MSE function is as follow [41]:

$$MSE = \frac{1}{N}\sum_{i=1}^{N}\left(Y_{pre} - Y_{ex}\right)^2 \quad (4)$$

Where Y_{ex} is the experimental output, Y_{pre} is the network output and N is the number of data points.

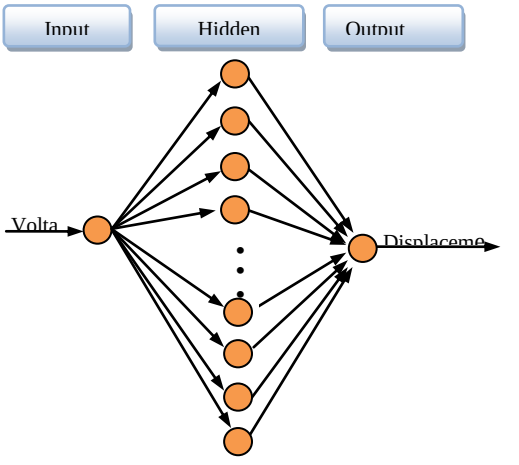

Fig. 9 The topology of optimized artificial neural network

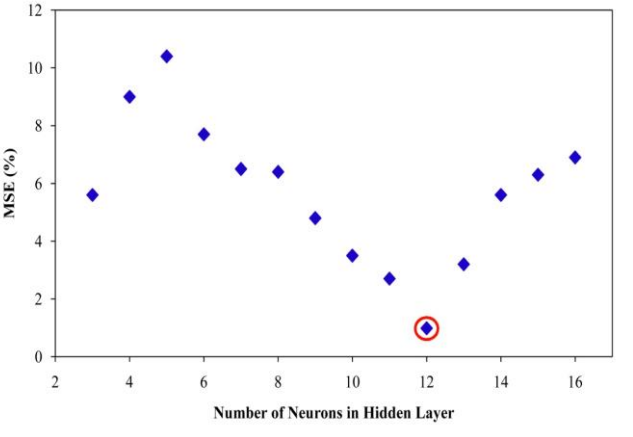

Fig. 10 The mean square error based on variation of neurons in hidden layer

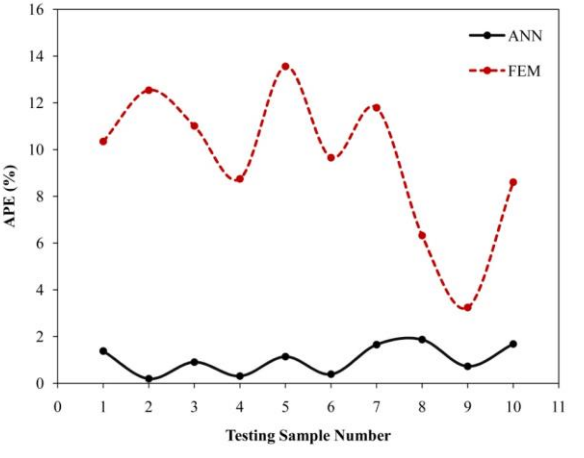

Fig. 11 MAPE of ANN and FEM versus experimental data points

The accuracy of ANN was examined by random selection of data from experimental data using test data set (Table 5). The values of absolute percentage error (APE) of each output reveal that the ANN was trained successfully and produced more accurate results. Moreover, the mean absolute percentage error (MAPE) of ANN and FEM were acquired 1.02 % and 9.58 % respectively which demonstrate high accuracy of the ANN model. Fig. 11 shows absolute percentage error of ANN and FEM models Vis-A-Vis experimental data set. The APE of predicted values by FEM model is more than ANN model, so the accuracy of ANN is higher than FEM model which is due to the high ability and potential of the ANNs to simulate and predict the nonlinear and non-model base relations.

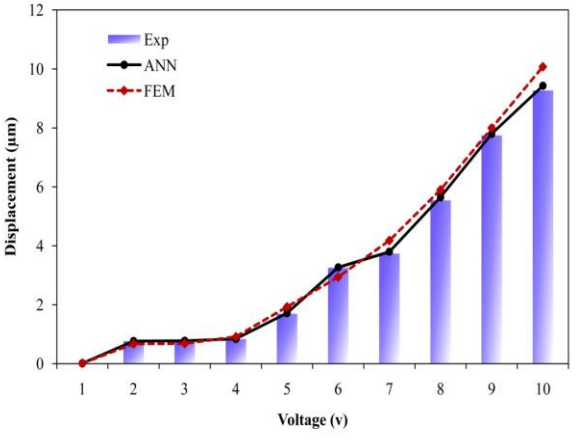

Fig. 12 The displacement of the arm hold versus applied voltage for experimental, ANN, and FEM results

As shown in Fig. 12, the displacement values of the arm hold illustrate versus applied voltage based on experimental, artificial neural network, and finite element results. Due to the small variations of the displacement in low voltages (i.e. less than 5 volts), the values of the displacement of the arms did not change significantly. However, for the voltages higher than 7 V (≥7 V), the displacement of the tip of the arms increases effectively with about the rate of 2 micrometers/volt.

As expected, the displacements of each arm in the finite element solution method (Except for three cases) are greater than the amount of experimental investigation which could be due to the following reasons:

a) Since in the solution of finite element analysis, structural mass (and damping of the air) is neglected, therefore structural displacement in the experimental condition will be less than the value obtained by the finite element method.

b) Manufacturing mistakes, lack of uniformity in the use of silicon and the changes of silicon properties due to the manufacturing process, are the main reasons of the mismatch of two graphs.

The amount of P-value (less than 0.05) indicates the good performance between the simulation and experimental results. The equipment setup is shown in Figure 13 and the results of t-tests are shown in table 6. The microgripper has more thermal and voltage tolerance compared to other electrothermal microgripper [22], [42], [43]. Furthermore, the obtained amount of tip displacement for voltage changes is acceptable [43].

Table 4 Train data points

Voltage (V)	Displacement (µm)									
1	0.015	0.045	0.015	0.005	0.005	0.005	0.015	0.005	0.02	0.015
2	0.74	0.765	0.75	0.765	0.75	0.74	0.755	0.87	0.765	0.795
3	0.765	0.765	0.865	0.74	0.745	0.74	0.74	0.82	0.72	0.82
4	1.848	1.792	1.792	0.172	0.177	0.172	0.228	0.228	1.853	0.152
5	1.384	1.217	1.207	1.016	2.628	1.217	1.22	2.636	2.428	2.033
6	2.532	1.923	2.864	3.928	3.848	2.93	3.65	3.64	3.64	3.6
7	3.124	4.280	4.690	4.17	3.495	3.44	3.853	3.46	3.22	3.65
8	5.69	5.236	5.960	6.014	5.028	5.72	5.604	5.498	5.823	4.89
9	7.68	7.693	7.78	8.003	7.936	7.722	7.794	7.47	7.53	7.83
10	9.205	9.425	9.2	9.2	9.205	9.425	9.3	9.205	9.205	9.37

Table 5 Comparative results of the experiment and predicted values by ANN for test data set

Factor		Displacement				
No.	Voltage	Exp	ANN	APE (%)	FEM	APE (%)
1	1	0.015	0.015	1.38	0.016	10.34
2	2	0.770	0.768	0.19	0.673	12.54
3	3	0.772	0.779	0.91	0.687	11.01
4	4	0.841	0.844	0.31	0.915	8.75
5	5	1.699	1.718	1.14	1.929	13.56
6	6	3.256	3.269	0.39	2.942	9.65
7	7	3.738	3.800	1.65	4.179	11.79
8	8	5.546	5.650	1.87	5.897	6.32
9	9	7.744	7.800	0.73	7.995	3.24
10	10	9.274	9.430	1.68	10.072	8.60
		MAPE (%)		1.02		9.58

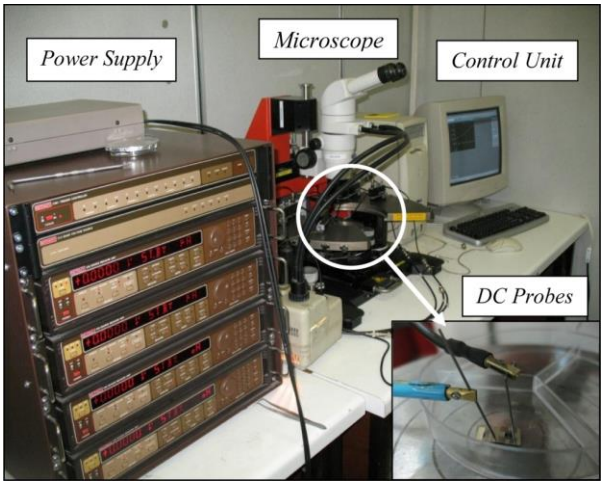

Fig. 13 Experiment equipment for measuring deflection

In this study, the measurement of the temperature distribution of the microgripper arms could not be achieved experimentally by variation of voltage. The reason refers to very small dimensions of arms, lack of a suitable non-contact temperature measurement device and also any touching of the probe with the microgripper arms to measure the temperature of the arms, may lead to the damage of the arms. For the same reasons, the optical and laser measuring devices cannot be used. Finally, a specified and exact temperature for arms cannot be considered. Consequently, the simulation of the temperature of the microgripper arms can be very useful. The movements of the tip of the microgripper arms are influenced by the selected thermal boundary conditions. As shown in Fig. 13, in both experimental and simulated results, with the increment of the applied input voltage, the total displacement of the arms grow moderately.

Table 6 T-test: Paired Two Sample for Means

	Experimental	FEM
Mean	3.36585	3.54220
Variance	10.31990034	11.60591862
Observations	10	10
Pearson Correlation	0.996455705	
Hypothesized Mean Difference	0	
df	9	
t Stat	-1.642154995	
P(T<=t) one-tail	0.067487018	
t Critical one-tail	1.833112933	
P(T<=t) two-tail	0.134974037	
t Critical two-tail	2.262157163	

4 CONCLUSIONS

In this work, a U-shape microgripper with electrothermal actuator was fabricated using vertical

and chemical etching methods. Then, the numerical solution of the microgripper arms displacements has been performed using COMSOL Multiphysics powerful finite element software. In this simulation, the maximum displacement of the end of the microgripper, for each arm was 10.072 µm. Moreover, the maximum temperature in hot (thin) arm was 497°K in the voltage of 10 V. The microgripper has more thermal and voltage tolerance compared to other electrothermal microgripper. Furthermore, the obtained amount of tip displacement for voltage changes is acceptable.

To verify the performance of the microgripper and the results of the simulations, the movements of the microgripper arms were tested experimentally and finally using paired t-test, good agreement between simulation and experimental investigation was obtained. Artificial neural network was applied successfully to predict the process with mean absolute percentage error of 1.02% and the determination coefficient (R2) of 0.9995. The results obtained from ANN and FEM showed that ANN model was more powerful and capable than FEM in prediction of arms hold displacement due to the lower mean absolute percentage errors, time consuming and low cost condition.

ACKNOWLEDGMENTS

The authors would like to thank Dr. Mehran Moradi, for his help in developing the idea of the work. They also like to appreciate Dr. Yaser Abdi for his kindly help in microgripper fabrication.

REFERENCES

[1] Kim, B.-S., Park, J.-S., Kang, B. H., And Moon, C., "Fabrication And Property Analysis of a MEMS Micro-Gripper for Robotic Micro-Manipulation", Robotics And Computer-Integrated Manufacturing, Vol. 28, 2012, Pp. 50-56.

[2] Lu, J., Kuwabara, H., Kurashima, Y., Zhang, L., and Takagi, H., "Optimization And Evaluation of the Size-Free Integration Process For MEMS-IC Assembly With High Yields And High Efficiency", Microelectronic Engineering, Vol. 145, 2015, Pp. 75-81.

[3] Yahiaoui, R., Zeggari, R., Malapert, J., and Manceau, J.-F., "A MEMS-Based Pneumatic Micro-Conveyor for Planar Micromanipulation", Mechatronics, Vol. 22, 2012, Pp. 515-521.

[4] Garcés-Schröder, M., Leester-Schädel, M., Schulz, M., Böl, M., And Dietzel, A., "Micro-Gripper: a New Concept for a Monolithic Single-Cell Manipulation Device", Sensors And Actuators A: Physical, Vol. 236, 2015, Pp. 130-139.

[5] Kivi, A. R., Azizi, S., "on The Dynamics Of A Micro-Gripper Subjected to Electrostatic and Piezoelectric Excitations", International Journal of Non-Linear Mechanics, Vol. 77, 2015, Pp. 183-192.

[6] Vijayasai, A. P., Sivakumar, G., Mulsow, M., Lacouture, S., Holness, A., Dallas, T. E., and Member, I., "Haptic Controlled Three Degree-Of-Freedom Microgripper System For Assembly of Detachable Surface-Micromachined MEMS", Sensors and Actuators A: Physical, Vol. 179, 2012, Pp. 328-336.

[7] Xia, X., Du, H., Wong, Y., And Yuan, Y., "Deposition And Characterisation of Shear-Mode Zno Sensor and Micro-Cantilever For Contact Sensing and Nanoactuation", Materials & Design, Vol. 93, 2016, Pp. 255-260.

[8] Zubir, M. N. M., Shirinzadeh, B., And Tian, Y., "A New Design of Piezoelectric Driven Compliant-Based Microgripper for Micromanipulation", Mechanism and Machine Theory, Vol. 44, 2009, Pp. 2248-2264.

[9] Kim, S., Zhang, X., Daugherty, R., Lee, E., Kunnen, G., Allee, D. R., Forsythe, E., and Chae, J., "Design and Implementation of Electrostatic Micro-Actuators In Ultrasonic Frequency on A Flexible Substrate, PEN (Polyethylene Naphthalate)", Sensors and Actuators A: Physical, Vol. 195, 2013, Pp. 198-205.

[10] Lai, H.-Y., Hsu, C.-H., And Chen, C.-K., "Optimal Design And System Characterization of Graphene Sheets In A Micro/Nano Actuator", Computational Materials Science, Vol. 117, 2016, Pp. 478-488.

[11] Chow, J., Lai, Y., "Displacement Sensing of a Micro-Electro-Thermal Actuator Using a Monolithically Integrated Thermal Sensor", Sensors And Actuators A: Physical, Vol. 150, 2009, Pp. 137-143.

[12] Wang, Z., Shen, X., And Chen, X., "Design, Modeling, and Characterization of a MEMS Electrothermal Microgripper", Microsystem Technologies, Vol. 21, 2015, Pp. 2307-2314.

[13] Yang, J., Lau, G., Tan, C., Chong, N., Thubthimthong, B., And He, Z., "An Electro-Thermal Micro-Actuator Based on Polymer Composite for Application to Dual-Stage Positioning Systems of Hard Disk Drives", Sensors And Actuators A: Physical, Vol. 187, 2012, Pp. 98-104.

[14] Lv, X., Wei, W., Mao, X., Chen, Y., Yang, J., And Yang, F., "A Novel MEMS Electromagnetic Actuator With Large Displacement", Sensors and Actuators A: Physical, Vol. 221, 2015, Pp. 22-28.

[15] Zhang, T., Zhang, P., Li, H.-W., Wu, Y.-H., And Liu, Y.-S., "Fabrication of Micro Electromagnetic Ectuator of High Energy Density", Materials Chemistry and Physics, Vol. 108, 2008, Pp. 325-330.

[16] Zhi, C., Shinshi, T., Saito, M., and Kato, K., "Planar-Type Micro-Electromagnetic Actuators Using Patterned Thin Film Permanent Magnets and Mesh Type Coils", Sensors and Actuators A: Physical, Vol. 220, 2014, Pp. 365-372.

[17] Michael, A., Kwok, C., "Piezoelectric Micro-Lens Actuator", Sensors and Actuators A: Physical, Vol. 236, 2015, Pp. 116-129.

[18] Hamedi, M., Salimi, P., and Vismeh, M., "Simulation And Experimental Investigation of a Novel Electrostatic Microgripper System", Microelectronic Engineering, Vol. 98, 2012, Pp. 467-471.

[19] Bazaz, S. A., Khan, F., And Shakoor, R. I., "Design, Simulation And Testing of Electrostatic SOI Mumps Based Microgripper Integrated With Capacitive Contact

Sensor", Sensors and Actuators A: Physical, Vol. 167, 2011, Pp. 44-53.

[20] Liu, G., Zhang, Y., Liu, J., Li, J., Tang, C., Wang, T., and Yang, X., "An Unconventional Inchworm Actuator Based on PZT/Erfs Control Technology", Applied Bionics And Biomechanics, Vol. 2016, Pp. 9.

[21] Singh, J., Teo, J., Xu, Y., Premachandran, C., Chen, N., Kotlanka, R., Olivo, M., and Sheppard, C., "A Two Axes Scanning SOI MEMS Micromirror for Endoscopic Bioimaging", Journal Of Micromechanics And Microengineering, Vol. 18, 2007, Pp. 025001.

[22] Pahwa, T., Gupta, S., Bansal, V., Prasad, B., and Kumar, D., "Analysis & Design Optimization of Laterally Driven Poly-Silicon Electro-Thermal Micro-Gripper for Micro-Objects Manipulation", In COMSOL Conf. Bangalore, 2012.

[23] Chong, S., Rui, S., Jie, L., Xiaoming, Z., Jun, T., Yunbo, S., Jun, L., And Huiliang, C., "Temperature Drift Modeling of MEMS Gyroscope Based on Genetic-Elman Neural Network", Mechanical Systems And Signal Processing, Vol. 72–73, 5// 2016, Pp. 897-905.

[24] El-Rabbany, A., El-Diasty, M., "An Efficient Neural Network Model for De-Noising of MEMS-Based Inertial Data", The Journal of Navigation, Vol. 57, 2004, Pp. 407-415.

[25] Fei, J., Wu, D., "Adaptive Control of MEMS Gyroscope Using Fully Tuned RBF Neural Network", Neural Computing And Applications, 2015, Pp. 1-8.

[26] Fontanella, R., Accardo, D., Caricati, E., Cimmino, S., And Simone, D. D., "An Extensive Analysis for The Use of Back Propagation Neural Networks to Perform The Calibration of MEMS Gyro Bias Thermal Drift", In 2016 IEEE/ION Position, Location and Navigation Symposium (PLANS), 2016, Pp. 672-680.

[27] Yan, W., Hou, S., Fang, Y., and Fei, J., "Robust Adaptive Nonsingular Terminal Sliding Mode Control of MEMS Gyroscope Using Fuzzy-Neural-Network Compensator", International Journal of Machine Learning And Cybernetics, 2016, Pp. 1-13.

[28] Mehrabian, A. R., Yousefi-Koma, A., "A Novel Technique for Optimal Placement of Piezoelectric Actuators on Smart Structures", Journal of The Franklin Institute, Vol. 348, 2011, Pp. 12-23.

[29] Rabenorosoa, K., Clévy, C., Lutz, P., Das, A. N., Murthy, R., And Popa, D., "Precise Motion Control of a Piezoelectric Microgripper for Microspectrometer Assembly", In ASME 2009 International Design Engineering Technical Conferences and Computers And Information In Engineering Conference, 2009, Pp. 769-776.

[30] Dang, X., Tan, Y., "RBF Neural Networks Hysteresis Modelling for Piezoceramic Actuator Using Hybrid Model", Mechanical Systems and Signal Processing, Vol. 21, 2007, Pp. 430-440.

[31] Dong, R., Tan, Y., Chen, H., And Xie, Y., "A Neural Networks Based Model for Rate-Dependent Hysteresis for Piezoceramic Actuators", Sensors and Actuators A: Physical, Vol. 143, 2008, Pp. 370-376.

[32] Luo, J., Fu, Y., Williams, J., And Milne, W., "Thermal Degradation of Electroplated Nickel Thermal Microactuators", Microelectromechanical Systems, Journal of, Vol. 18, 2009, Pp. 1279-1287.

[33] Comsol, M., Femlab, R., "Module Model Library", COMSOL Multiphysics®, Version, Vol. 3, 2005,

[34] Mankame, N. D., Ananthasuresh, G., "Comprehensive Thermal Modelling And Characterization of An Electro-Thermal-Compliant Microactuator", Journal Of Micromechanics And Microengineering, Vol. 11, 2001, Pp. 452.

[35] Hamedi, M., Vismeh, M., And Salimi, P., "A New MEMS Assembly Unit for Hybrid Self Micropositioning and Forced Microclamping of Submilimeter Parts", In Advanced Materials Research, 2011, Pp. 1705-1712.

[36] Shakeri, S., Ghassemi, A., Hassani, M., And Hajian, A., "Investigation of Material Removal Rate and Surface Roughness In Wire Electrical Discharge Machining Process For Cementation Alloy Steel Using Artificial Neural Network", the International Journal of Advanced Manufacturing Technology, Vol. 82, 2016, Pp. 549-557.

[37] Leema, N., Radha, P., Vettivel, S. C., And Khanna Nehemiah, H., "Characterization, Pore Size Measurement And Wear Model of a Sintered Cu–W Nano Composite Using Radial Basis Functional Neural Network", Materials & Design, Vol. 68, 3/5/ 2015, Pp. 195-206.

[38] Xia, X., Nie, J. F., Davies, C. H. J., Tang, W. N., Xu, S. W., And Birbilis, N., "An Artificial Neural Network for Predicting Corrosion Rate and Hardness of Magnesium Alloys", Materials & Design, Vol. 90, 1/15/ 2016, Pp. 1034-1043.

[39] Salehi, I., Shirani, M., Semnani, A., Hassani, M., and Habibollahi, S., "Comparative Study Between Response Surface Methodology and Artificial Neural Network for Adsorption of Crystal Violet on Magnetic Activated Carbon", Arabian Journal for Science And Engineering, 2016, Pp. 1-11.

[40] Shirani, M., Akbari, A., and Hassani, M., "Adsorption of Cadmium (Ii) And Copper (Ii) From Soil and Water Samples onto a Magnetic Organozeolite Modified With 2-(3, 4-Dihydroxyphenyl)-1, 3-Dithiane Using An Artificial Neural Network and Analysed By Flame Atomic Absorption Spectrometry", Analytical Methods, Vol. 7, 2015, Pp. 6012-6020.

[41] Jenab, A., Sari Sarraf, I., Green, D. E., Rahmaan, T., and Worswick, M. J., "The Use of Genetic Algorithm and Neural Network to Predict Rate-Dependent Tensile Flow Behaviour of AA5182-O Sheets", Materials & Design, Vol. 94, 3/15/ 2016, Pp. 262-273.

[42] Krecinic, F., Duc, T. C., Lau, G., And Sarro, P., "Finite Element Modelling and Experimental Characterization of an Electro-Thermally Actuated Silicon-Polymer Micro Gripper", Journal of Micromechanics and Microengineering, Vol. 18, 2008, P. 064007.

[43] Paryab, N., Jahed, H., And Khajepour, A., "Creep and Fatigue Failure In Single-And Double Hot Arm MEMS Thermal Actuators", Journal of Failure Analysis and Prevention, Vol. 9, 2009, Pp. 159-170.